Journal of the Physical Society of Japan
Vol. 68, No. 10, October, 1999, pp. 3248-3253

Electron Capture Cross Sections of H(2p) Level in the Intermediate Velocity Regime of H^+–Na(3s), Na^*(3p) Collisions

Rei OKASAKA, Shin ASADA, Kazuyoshi NAEMURA, Yoshiho SEO, Satoshi TOJO and Yasuo MATSUMURA

Department of Mechanical Physics, Kyoto University, Kyoto 606-8501

(Received March 29, 1999)

We measured electron capture cross sections of H(2p) level as functions of collision velocity by the observation of Lyman-α line emitted from decaying H(2p) atoms, in H^+–Na(3s), and –Na^*(3p) collisions. Excited sodium atoms were generated by optical excitation with a tunabe dye-laser and the energy of incident protons was in the range of 1–16 keV. The measured results are consistent with previous experiments if they exist and with theoretical calculations. The characteristic dependences on collision velocity of the cross sections were reproduced by the velocity-matching model in which the characteristics of the intermediate velocity collision were taken into account.

KEYWORDS: proton sodium collision, intermediate velocity regime, electron capture cross section, laser excitation, Lyman-α line

§1. Introduction

In the intermediate velocity regime of ion-atom collisions electron capture cross sections show various behaviors as functions of collision velocity, sensitively responding the change of collision velocity. Thus we can infer that a behavior of electron capture cross section reflects characteristics of the momentum distribution of the electronic orbitals captured.[1] In the same way characteristics of the momentum state of the initial orbitals in a target-atom may affect a behavior of electron capture cross section. The ground state of a usual monoatomic target is the S-state. In order to study the characteristics of electron capture process from a non-S state atom, we have to produce a sufficient quantity of the non-S state target atom.

In the present experiment, we generated excited-state target atoms by irradiation of laser light on a sodium beam effusing from an aperture of a sodium oven. By spectroscopic measurement on Lyman-α line emitted from decaying H(2p), we determined the electron capture cross sections to H(2p) level in H^+–Na(3s) and H^+–Na^*(3p) collisions. Some of the measured cross sections were compared with the previous results measured by other authors.

A sodium atom can be treated by a quasi-one-electron-atom approximation and this feature brings fair advantage in calculation of electron capture cross sections. Comparisons of the measured results with those of calculations based on the close-coupling method by others were made in H^+–Na(3s) and –Na^*(3p) collisions. The behaviors of measured electron capture cross sections to H(2p) level are also examined by those using the velocity matching model proposed by us previously.[2]

§2. Experimental Set-Up

2.1 Proton beam and sodium beam

Figure 1 shows a schematic diagram of the experimental apparatus. Protons from a duoplasmatron ion-source are accelerated to an energy in the range of 1–16 keV and selected by an analysing magnet.[3] The proton beam current is about 0.5 μA(1 keV)–30 μA(16 keV). The ion beam is collimated with two hole-slit of 3 mm diameter. The background pressure of the collision chamber is less than 1.0×10^{-6} Torr.

The sodium beam effusing from an aparture of 1 mm diameter at the upside of an oven cell (Fig. 2) is limited by a water-cooled heat-shield within 1° in effusing angle. The temperature of the oven is about 350°C and the ratio of Na_2 in the sodium vaper is less than 1.5%.[4] The sodium beam is adsorbed with a liquid-nitrogen trap equipped above the oven.

2.2 Laser excitation of sodium beam

The laser light of λ589.0 nm from a ring dye laser (Coherent CR699-21 using Rhodamine 6G) excited by an argon-ion laser (Coherent I-100-18) excites sodium atoms to Na($3p^2P_{3/2}F$=3) level (Fig. 3). The laser light, the atomic beam and the ion beam cross in rightangle with each other.

The oscillation frequency of the laser light shifts with time. Thus, we installed the reference cavity equipped with a sodium heat-pipe oven to identify the frequency of excitation with a sharp Doppler-free spectrum generated by a saturation spectroscopy method (Figs. 4(a) and 4(b)). We detected the shift of the laser light from the reference line and tried to fix the frequency of the dye laser oscillation by a feedback circuit. The variation of the frequency was controlled within 10 MHz for few hours by this system.

The excitation of a sodium atom by λ589.0 nm

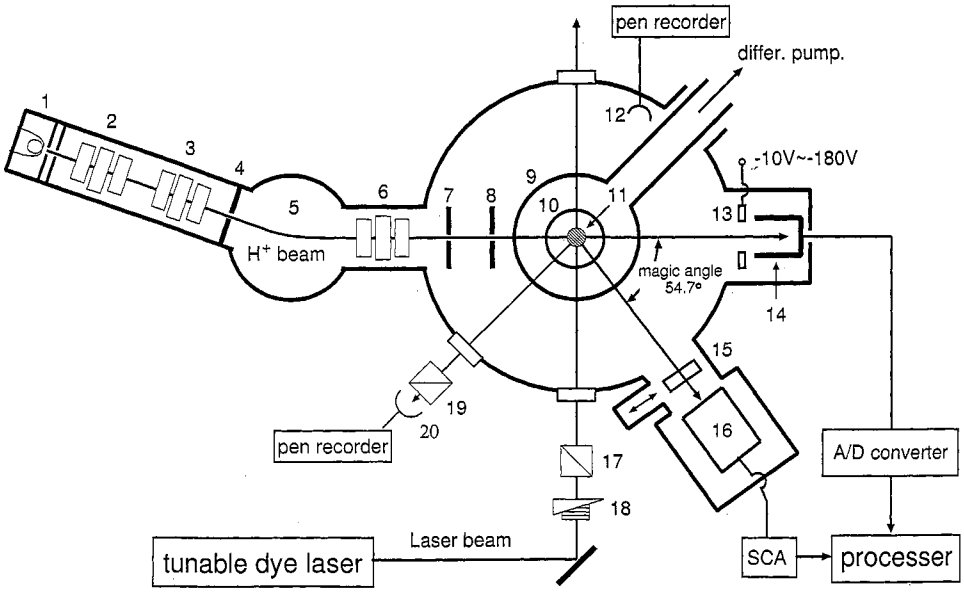

Fig. 1. Schematic diagram of apparatus. 1: duoplasmatron ion source. 2, 3: Einzel lenses. 4: aperture. 5: analyzing magnet. 6: Einzel lense. 7,8: apertures. 9: heat shield. 10: sodium oven. 11: sodium beam. 12: photo-diode. 13: secondary electron supresser. 14: Faraday cup. 15: MgF_2 window. 16: photomultiplier(R595). 17: polarizer. 18: Soleil-Babinet's compensator. 19: polarizer. 20: photo-diode. SCA: single channel analyzer.

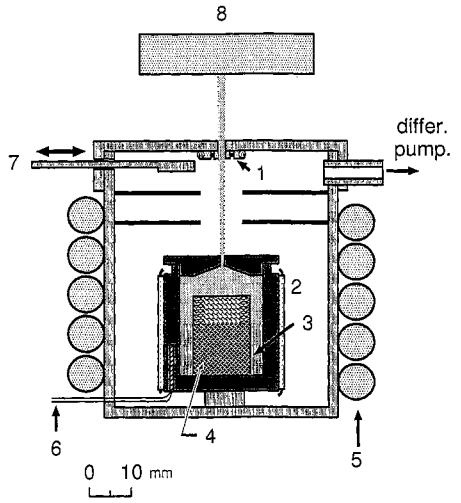

Fig. 2. Sodium oven and heat shield. 1, 2: heaters. 3: metalic sodium. 4: stainless-mesh wick. 5: cooling-water pipe. 6: thermocouple. 7: shutter. 8: liquid-nitrogen trap.

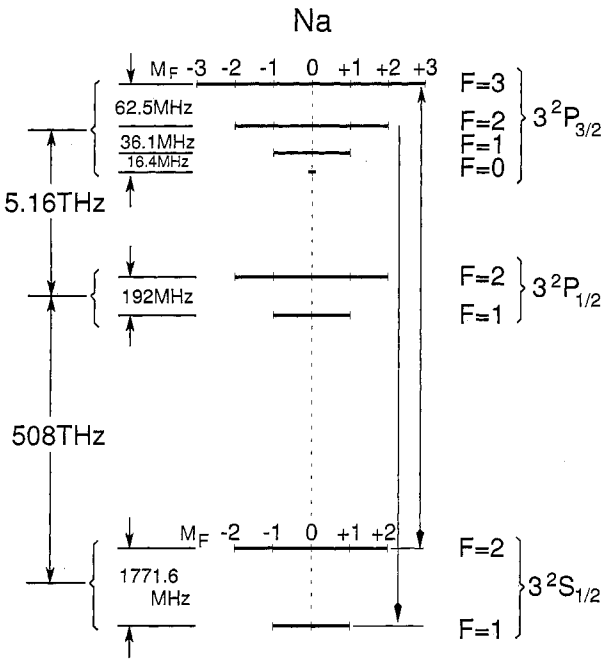

Fig. 3. Energy level diagram of Na D_1 and D_2 lines.

line (D_2: $3s^2S_{1/2}F=2 \rightarrow 3p^2P_{3/2}F=3$) irradiation forms seemingly a two-level system, because the transition of $3p^2P_{3/2}F=3 \rightarrow 3s^2S_{1/2}F=2$ is only one optically-allowed transition from $3p^2P_{3/2}F=3$ level. The statistical ratio of $3s^2S_{1/2}F=2$ level against all the ground state levels is 5/8 and, so that, the theoretical excitation fraction is expected of 0.31 in the saturated state. However, the mixing of the hyperfine levels of $3p^2P_{3/2}F=3$ with $3p^2P_{3/2}F=2$ levels caused by line broadening effects, such as power broadening and Doppler broadening, generates another transition of $3p^2P_{3/2}F=2 \rightarrow 3s^2S_{1/2}F=1$, which gives rise to the accumulation of sodium atoms to the $3s^2S_{1/2}F=1$ level. The mechanism mentioned above and many other reasons reduce the fraction f of the excited Na*(3p) level. In the present experiment, direct measurement of f was not performed and the fration of 0.1 was estimated from the comparison of the conditions of the laser irradiation with those of the previous experiment[5-7] in which an absolute measurement of f had been done.

2.3 *Spectroscopic measurement*

Lyman-α radiation from decaying H(2p) level was detected by a electron multiplier (Hamamatsu Photonics R595); the first dynode of a R595 electron multiplier is made of BeCuO and we can use the tube as a photomultiplier to a vacuum ultra violet (VUV) radiation less than λ130 nm (Fig. 5). A MgF_2 window absorbs the radiation shorter than λ110 nm and, so that, the window

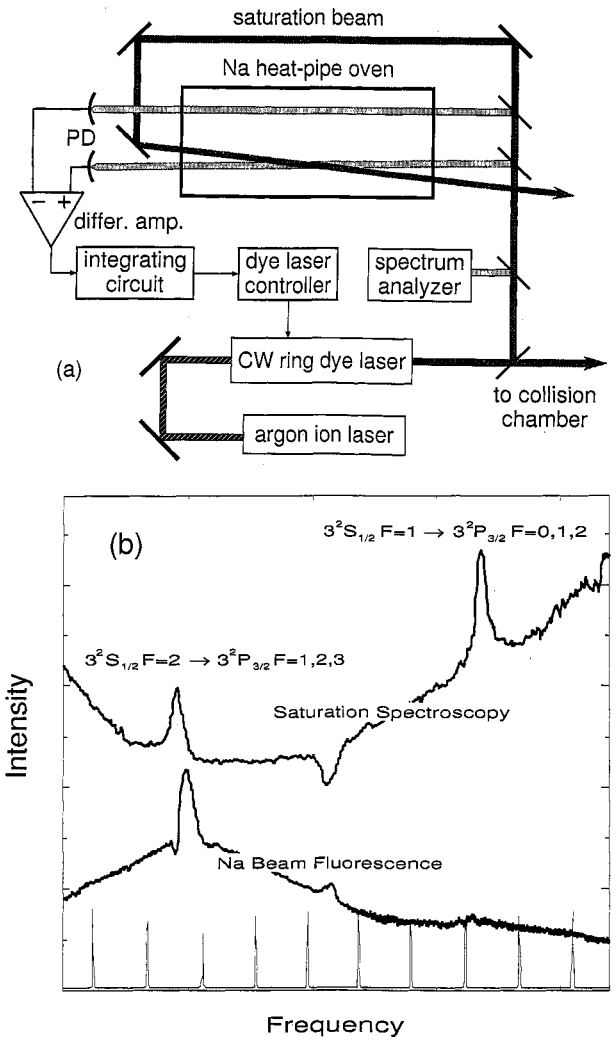

Fig. 4. Saturation spectroscopy of Na D_2 lines. (a) Schematic diagram of apparatus and (b) Doppler-free spectra of D_2 lines (top trace), the fluorescence of laser-excited sodium beam (middle trace) and the output of spectrum analyzer (bottom trace). The free spectral range of spectrum analyzer was 300 MHz. The frequency of excitation laser was scanned. In the measurement of laser-excited beam, the frequency of dye laser was locked at the high-frequency-side slope of the Doppler free spectra of the $3^2S_{1/2}F = 2 \rightarrow 3^2P_{3/2}F = 1, 2, 3$ transitions.

acts as a filter for a Lyman-α line at a combination with R595 in the present experiment. The direction of the observation is 54.7° (magic angle) against the ion beam axis. Thus the observed intensity of the Lyman-α line is proportional to the electron capture cross section of H(2p) level.

The photo-diode equipped with the polarizer, of which the polarization axis is paralell or perpendicular to the plane composed of the direction of the polarization axis of the laser light and the direction of the observation, measures the intensity of the fluorescence of the sodium atom excited by the linearly polarized laser-light. A shutter is installed on each path of the ion beam, the atomic beam and the laser light and various synchronous on-off measurements were performed.

First the electron capture cross section of H(2p) level in H^+–Na(3s) collision without the laser excitation ($\sigma_{3s}(2p)$) was measured by the observation of the intensity of the Lyman-α line emitted from the hydrogen atom

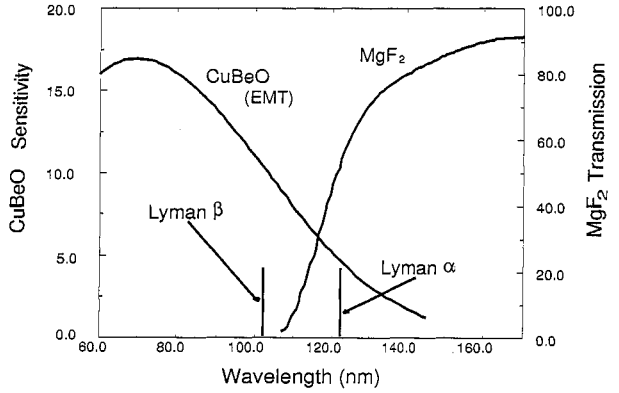

Fig. 5. Sensitivity of CuBeO and transmission of MgF_2 window.

that captured an electron from Na(3s). Next apparent electron capture cross section of H(2p) level ($\sigma^*(2p)$) was measured for the laser-excited sodium beam. The relation among $\sigma^*(2p)$, $\sigma_{3s}(2p)$) and $\sigma_{3p}(2p)$ is

$$\sigma^*(2p) = (1-f)\sigma_{3s}(2p) + f\,\sigma_{3p}(2p),$$

where $\sigma_{3p}(2p)$ is the electron capture cross section to H(2p) level in H^+–$Na^*(3p)$ collision and f is the excitation fraction of Na(3p) level in the sodium beam.

§3. $Na^*(3p)$ Excited by a Linearly Polarized Light

We excited sodium atoms by the linearly polarized laser-light of which the wavelength was equal to the Na D_2 line ($3s\ ^2S_{1/2}\ F_l$=2–$3p^2P_{3/2}F_u$=3). The polarization direction of the laser light was taken as the quantum axis. The intensity of fluorescence from the excited atoms is shown as follows:[8]

$$I = n_e C\{1+\frac{1}{4}g^{(2)}[1-3\cos^2\Theta+3\sin^2\Theta\cos 2\Psi\cos 2\beta]a_0 + \frac{3}{2}g^{(1)}\cos\Theta\sin 2\beta\cdot o_0\}, \quad (3.1)$$

where n_e is number of excited atoms, C is the constant containing detection efficiency and total transition probability, Θ is the angle between the quantum axis and the direction of observation, Ψ is the angle between the plain composed of the quantum axis and the observation direction and the polarization plain of the observing light, a_0 is an alignment parameter. An orientation parameter o_0 is equal to 0 in the case of excitation by a linearly polarized light and $g^{(k)}$ is the HFS-recoupling coefficient of rank k for light emission from a single transition $F_u \rightarrow F_l$ given as follows with 3-j symbols:

$$g^{(2)} = (-1)^{F_u-F_l}[F_u(F_u+1)]^{-1} \begin{Bmatrix} F_u & F_u & k \\ 1 & 1 & F_l \end{Bmatrix} \Big/ \begin{Bmatrix} F_u & F_u & k \\ 1 & 1 & F_u \end{Bmatrix}. \quad (3.2)$$

The phase of excitation light β is given as follows:[9]

$$\beta = \begin{cases} 0 & \text{linearly polarized light,} \\ +\pi/4 & \text{right-handed circularly polarized light,} \\ -\pi/4 & \text{left-handed circularly polarized light.} \end{cases}$$

In this case of $F_u = 3$ and $F_l = 2$, $g^{(2)}$ is $-1/15$. The alignment parameter of electronic state $a_0(L)$ of the case of $F_u = 3$, $J_u = 3/2$, $I_u = 3/2$, $S_u = 1/2$ and $L_u = 1$ is

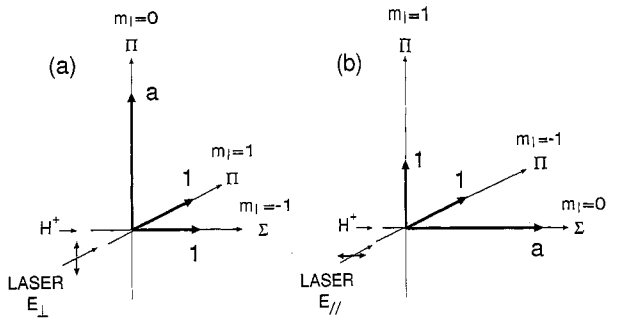

Fig. 6. Populations of magnetic sublevels of Na(3p) and populations in molecular description, excited by linearly polarized light. Excitation was performed with the polarized light paraiell (a) and perpendicular (b) to the plane defined by the ion-beam axis and the observation direction.

given as $a_0(L) = a_0/15$.[8] The intensities of fluorescences of $I_{\Psi=0}$ and $I_{\Psi=\pi/2}$ at the observation of $\Psi = 0$ and $\Psi = \pi/2$, respectively, and the observation direction against the quantum axis $\Theta = \pi/2$ are shown as follows from eq. (3.1):

$$I_{\Psi=0} = n_e C\{1 + g^{(2)}a_0\} \tag{3.3}$$

$$I_{\Psi=\pi/2} = n_e C\{1 - g^{(2)}a_0/2\}. \tag{3.4}$$

Thus

$$a_0(L) = \frac{a_0}{15} = \frac{1}{15\,g^{(2)}} \frac{2(I_{\Psi=0} - I_{\Psi=\pi/2})}{(I_{\Psi=0} + I_{\Psi=\pi/2})}. \tag{3.5}$$

The alignment parameter $a_0(L)$ is shown with the population probabilities of magnetic sublevels $P(M_L)$ of $L = 1$:

$$a_0(L) = P(-1) + P(+1) - 2P(0), \tag{3.6}$$

$$P(-1) + P(+1) + P(0) = 1. \tag{3.7}$$

Therefore,

$$P(0) = 1/3 - a_0(L)/3, \tag{3.8}$$

$$P(\pm 1) = 1/3 + a_0(L)/6. \tag{3.9}$$

In the present experiment, the ratio of populations among the magnetic sublevels $p(3p_{M_L})$ was obtained by the observations of intensities of the linearly polarized fluorescences $I_{\Psi=0}$ and $I_{\Psi=\pi/2}$:

$$p(3p_{-1}) : p(3p_0) : p(3p_{+1}) = 1 : a : 1 = 1 : 1.94 : 1. \tag{3.10}$$

The relation between the populations of the quasi-molecular states formed at the collisional interaction $p(3p\Lambda)$, which are often used in a theoretical calculation, and $p(3p_{M_L})$ above mentioned is shown in Fig. 6. The direction of ion injection is taken as the molecular axis. When the excitation laser light is linearly polarized in the direction parallel to the ion-beam axis ($\|$),

$$p(3p\Sigma) : p(3p\Pi) = a : (1 + 1), \tag{3.11}$$

and in the direction perpendicular to the ion-beam axis ($\perp$),

$$p(3p\Sigma) : p(3p\Pi) = 1 : (1 + a). \tag{3.12}$$

Finally we obtain

$$\sigma_{3p\|} = \frac{1}{a+1}(a\ \sigma_{3p\Sigma} + 2\sigma_{3p\Pi}), \tag{3.13}$$

$$\sigma_{3p\perp} = \frac{1}{a+1}\{\sigma_{3p\Sigma} + (1+a)\sigma_{3p\Pi}\}, \tag{3.14}$$

where $\sigma_{3p\|}$ indicates the electron capture cross section of H(2p) level in collision with Na^*(3p) atom excited by the laser light polarized parallel to the ion-beam axis and so forth.

§4. Results and Discussion

The life time correction[10] for the Lyman-α intensity measurement is not necessary in the present experiment, because the size of the observation region is 15 mm contrary to short life time of H(2p) level of 1.5 ns.[11] The most effective contributions of the cascade effects from the upper levels are those from H($n = 3$) levels. Most of the optical decay of H(3s) level atom occurs out of the observation region because of long life time 158 ns of the level. The life time of H(3d) level is 15.5 ns and so that the cascade from H(3d) level affects measurement of electron capture cross section of H(2p) level at slow velocity collision in the intermediate velocity regime. We have no data about the cross section of H(3d) level and, however, the ratio between the electron capture cross section of H($n = 2$) level and the H($n \geq 3$) level in H^+–Na(3s) collision has been measured:[5]

$$\sigma_{3s}(n \geq 3)/\sigma_{3s}(n = 2) = 0.07 \quad (E = 3\ \text{keV}).$$

The rate of electron capture to the H($n \geq 3$) level is small and we can neglect the influence of the cascade effect on the discussion about the behavior of the electron capture cross section of the H(2p) level in the intermediate velocity regime.

The intensities of the Lyman-α line were measured in the energy range of 1–16 keV relatively. The electron capture cross section at the collision energy of 3 keV in H^+–Na(3s) collision was normalized to the result obtained by Gieler *et al.*[7] The measured electron capture cross sections of $\sigma_{3s}(2p)$ and $\sigma_{3p\perp}(2p)$ are shown in Fig. 7, together with the results obtained by Finck *et al.*[6] and Gieler *et al.*[7] The dependences of the cross sections on collision velocity agree with those of the previous measurements where data exist. The agreement of the relative intensities of $\sigma_{3s}(2p)$ and $\sigma_{3p\perp}(2p)$ throughout the measured energy range indicates that the estimated excitation fraction $f = 0.1$ is reasonable.

Figures 8 and 9 show the comparison of the present results with the calculations based on the close-coupling method by Fritsch[12] (AO bases) and Courbin *et al.*[13] (MO bases). The calculations reproduce the measured electron capture cross sections, on the whole.

We have proposed a simple model to describe the characteristics of the behaviors of electron capture cross sections in the intermediate velocity regime.[2] We introduced the velocity matching model, which holds for high velocity collisios, to our model for the intermediate velocity collisions. The deformation of the wavefunctions caused by the colliding particles during collision is neglected, in the model, to make clear the characteristics

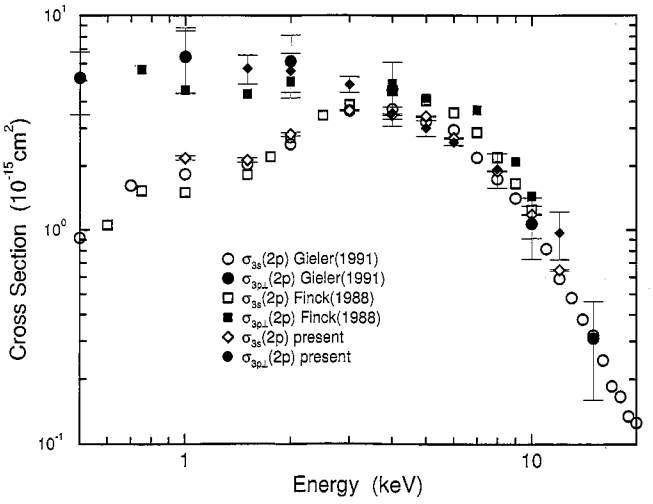

Fig. 7. Electron capture cross sections of the H(2p) level in H^+–Na(3s) and H^+–Na*(3p) collisions and experimental results by Finck *et al.*[6] and Gieler *et al.*[7] The symbol $3p_\perp$ indicates that the Na*(3p) atom is generated by the laser light polarized perpendicular to the plane defined by the ion-beam axis and the observation direction.

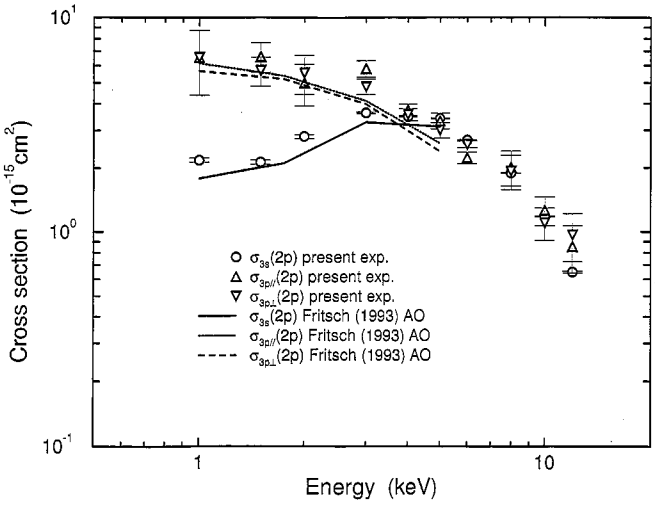

Fig. 8. Electron capture cross sections of the H(2p) level in H^+–Na(3s) and H^+–Na*(3p) collisions and the calculated results based on AO by Fritsch.[12]

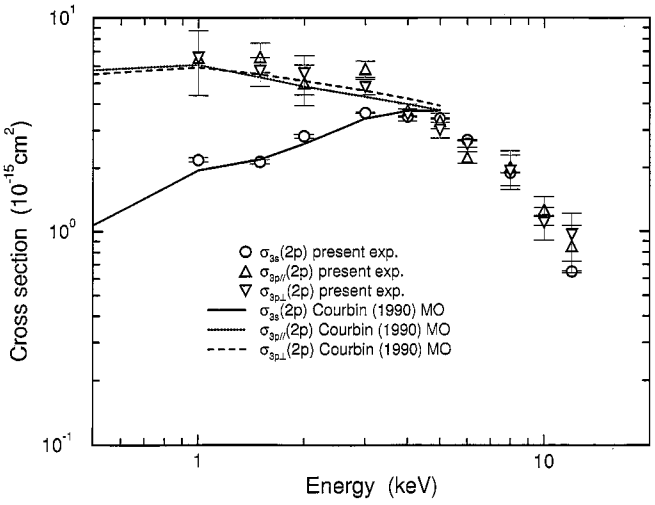

Fig. 9. Electron capture cross sections of the H(2p) level in H^+–Na(3s) and H^+–Na*(3p) collisions and the calculated results based on MO by Courbin *et al.*[13]

of the initial and final state wavefunctions and to simplify calculations. The transition probability of electron transfer is given by the overlapping integral of probability distribution of momentum of the initial and final states at the closest internuclear distance R_0 (=b: impact parameter), as follows in atomic unit:

$$P = \left| \int \psi'_{proj}(\boldsymbol{r} - \boldsymbol{R}_0)^* \psi_{targ}(\boldsymbol{r})\, \mathrm{e}^{\mathrm{i}m_e \boldsymbol{V}\cdot\boldsymbol{r}} \mathrm{d}\boldsymbol{r} \right|^2, \quad (4.1)$$

where m_e(=1) is electron mass, $\boldsymbol{r}$ is coordinate of an active electron, $\boldsymbol{V}$ is collision velocity and $\psi'_{proj}(\boldsymbol{r} - \boldsymbol{R}_0) = \psi_{proj}(\boldsymbol{r})$.

Measurements of differential electron capture cross sections of H(2s) level in H^+-H collisions[14] show that the maximum of the probability of electron capture arises at the collision of impact parameter less than the average distance of $1s$ electron from the nucleus of the target hydrogen atom in the intermediate velocity regime[2] and that the probability decreases rapidly with the increase of impact parameter. This characteristic of the intermediate velocity collision is introduced to the model as a cutoff function for impact parameter b:

$$f_{cutoff}(b) = \frac{(Q_0^2 - b^2)^{1/2}}{Q_0} \qquad b < Q_0, \quad (4.2)$$

where Q_0 is the averaged distance of an active electron from the nucleus of a target atom. Another characteristic that finite relaxation time necessary to an electron transfer process reduces the cross section proportionally to $1/V$, as collision velocity V increases, gives additional parameter V_0/V, where $V_0 = v_e/\pi$ and v_e is the averaged velocity of the active electron of target. Finally, the electron capture cross section σ is given by the following equation:

$$\sigma = C \int_0^{Q_0} \frac{V_0}{V} \frac{(Q_0^2 - b^2)^{1/2}}{Q_0} P\, 2\pi b\, \mathrm{d}b, \quad (4.3)$$

where C is an adjustable parameter determined by comparison with the measured cross sections. We use a fixed value of C for each collision system.

Approximate one-electron wavefunctions of sodium are necessary to apply the above model to H^+–Na(3s) and –Na*(3p) collisions. We assume that the electronic charge distribution of Z-1 inner-shell electrons is proportional to $\mathrm{e}^{-r/\alpha}$, where α is an undetermined parameter. The most outside electron moves in the potential field $V(r)$ produced by the inner shell electrons and the nucleus. First the Schrödinger equation of the ground state wavefunction of S-state is numerically solved and the parameter α is so determined as to coincide the energy of the ground state with the spectroscopic ionization potential. Then, retaining this value of α, the equation is integrated for the excited levels of sodium. Numerical wavefunctions are obtained corresponding to energies of the levels which have to be chosen so that $\phi_{nlm} \to 0$ as r $\to \infty$. The radial functions of 3s and 3p levels of sodium fitted by analytical functions are shown as follows in atomic unit:[15]

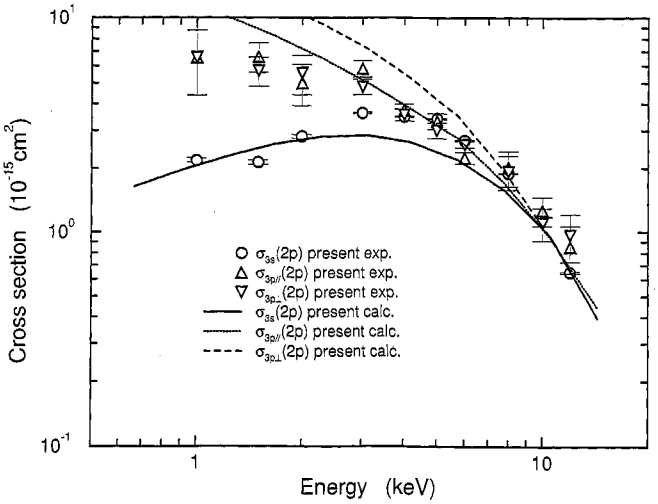

Fig. 10. Electron capture cross sections of the H(2p) level in H^+–Na(3s) and H^+–Na^*(3p) collisions and the results of the present calulations based on the velocity matching model. H^+–Na(3s): $V_0 = 0.73$ au (atomic unit), $Q_0 = 4.0$ au. H^+–Na^*(3p): $V_0 = 0.60$ au, $Q_0 = 5.7$ au. $C = 10$.

$$R_{3s}(r) = 0.702244\ (r - 0.961)\ [\ e^{-0.71r} - 14\ (0.34 - r)\ e^{-3.6r}\ ], \tag{4.4}$$

$$R_{3p}(r) = 0.148743r\ [\ 25.4\ e^{-3.8r} - e^{-0.44r}\ ]. \tag{4.5}$$

The normalized function is given below:

$$\phi_{nlm}(r, \theta, \phi) = R_{nl}(r) Y_l^m(\theta, \phi),$$

where $Y_l^m(\theta, \phi)$, n, l and m are in usual uses.

We calculated the electron capture cross section of the H(2p) level in H^+–Na(3s) and H^+–Na^*(3p) collisions, using the model above mentioned. The calculated results are shown in Fig. 10. In the energy range of 1–10 keV, which corresponds to the intermediate velocity regime of H^+–Na(3s), Na^*(3p) collisions, the calculated results reproduce the characteristics of the velocity depedence of the measured electron capture cross sections.

§5. Conclusion

It is desirable that a fraction of excited-state atom is large and stable in time on the measurement for the reaction of excited-state atoms. Optical excitation by a laser light is a powerful method to produce a sample of excited-state atom, though the state of the produced excited-atom is limited by the selection rule of the optical transition. In the present experiment, the fraction of excited-state atom was determined indirectly by comparison of the experimental conditions with those of the previous measurements. Good agreement of the present results with the results of the previous measurements for H^+–Na^*(3p) collision indicates that the laser-light irradiation is a sure and reliable method of the excited atom production.

We have found that electron capture cross sections and excitation cross sections show the characteristic dependences on collision velocity in the intermediate velocity regime.[1,2,16] The characteristics of electron capture cross section in the collision with an S-level atom were well reproduced by the model proposed by us,[2] in which the transition probability of electron transfer was given as the overlapping integral of wavefunctions in momentum space. It has been shown in the present studies that the model is applicable to the electron capture process for optically excited P-level atoms. This fact suggests that velocity matching in electron transfer process is not only the characteristic of high velocity collisions but also the characteristic of intermediate velocity collisions.

The limit of cutoff (Q_0) in eq. (4.2) gives considerable influence on the behavior of electron capture cross section given by eq. (4.3). The role of the cutoff function is important to describe the behavior of the measured cross section. The classical trajectory method indicates that a specified trajectory of an electron is needed for electron capturing closely relating to the trajectories of the projectile and target atom nuclei and that close collisions are effective in the intermediate velocity regime. We think that the mechanism of electron capture in the intermediate velocity regime is to include momentum conservation of the transferred electron, which is the characteristic of high velocity collisions, and dominance of close collision, which is the characteristic of low velocity collisions.

Our model explains only the behaviors of electron capture cross section, and does not give its absolute intensity. It is useful, however, to know the collision velocity corresponding maximum of cross section or even to know whether a maximum of the cross sections exists or not, for practical uses. A crude estimate of an electron capture cross section relative to cross sections to other levels is also obtained by the model. In the intermediate velocity collisions of a low-ionization-stage ion and a light atom, the levels to which electrons are dominantly captured are not so many. Appropriate selection of a target atom, we expect, makes possible to produce a beam including many excited atoms of the specified level. Above model may give a clue to the selection of excited target atoms.

1) R. Okasaka, K. Kawabe, S. Kawamoto, M. Tani, H. Kuma, T. Iwai, K. Mita and A. Iwamae: Phys. Rev. A **94** (1994) 995.
2) R. Okasaka, K. Mita, S. Asada, K. Naemura and Y. Seo: Jpn. J. Appl. Phys. **38** (1999) 244.
3) R. Okasaka, Y. Konishi, Y. Sato and K. Fukuda: J. Phys. B **20** (1987) 3771.
4) Richard E. Honing: RCA Review **23** (1962) 576.
5) T. Royer, D. Dowek, J. C. Houver, J. Pommier and N. Andersen: Z. Phys. D **10** (1988) 45.
6) K. Finck, Y. Wang, Z. Roller-Lutz and H. O. Lutz: Phys. Rev. A **38** (1988) 6115.
7) M. Gieler, F. Aumayr, M. Hütteneder and H. Winter: J. Phys. B **24** (1991) 4419.
8) A. Fischer and I. V. Hertel: Z. Phys. A **304** (1982) 103.
9) M. Born and E. Wolf: *Principles of Optics* (Pergamon Press, New York, 1970).
10) L. W. Muller and F. J. de Heer: Physica **48** (1970) 345.
11) H. A. Bethe and E. E. Salpeter: *Quantum Mechanics of One- and Two-Electron Atoms* (Plenum Publishing Corporation, New York, 1977).
12) W. Fritsch: Phys. Rev. A **30** (1984) 1135.
13) C. Courbin, R. J. Allan, P. Salas and P. Wahnon: J. Phys. B **23** (1990) 3909.
14) J. E. Bayfield: Phys. Rev. Lett. **25** (1970) 1.
15) D. Rapp and C. M. Chang: J. Chem. Phys. **58** (1973) 2657.
16) R. Okasaka, Y. Seo, S. Tojo and Y. Matsumura: Jpn. J. Appl. Phys. **38** (1999) 1564.